# CHAPTER -2

# Effect of normal and disrupted circadian rhythm on the mitochondria

## 1. Introduction

The circadian system in mammals is primarily entrained by the earth's 24 h light-dark (LD) cycle and regulates numerous physiological, behavioral, and metabolic processes on a systemic as well as a cellular level in a temporally appropriate manner (Albrecht et al., 1997; Tei et al.,1997; Do & Yau, 2010). This circadian system is a hierarchical network of oscillators located in the anterior hypothalamus suprachiasmatic nucleus (SCN). It receives direct information about the environmental LD cycle from the retina and coordinates with numerous subordinate oscillators in extra-SCN brain regions and peripheral tissues (Yamazaki et al., 2000; Yoo et al., 2004). This circadian clock allows organisms to respond predictably to changes in the external environment, such as food availability, and prepares cellular metabolism for suitable energy substrate selection, for example, glucose (during the active phase) and fatty acid (during the inactive phase) (Longo and Panda., 2016). Such periodic changes in energy supply and energy demand are regulated by mitochondria (Neufeld-Cohen et al., 2016; P. de Goede et al., 2022).

Panda et al., 2002 reported more than 300 genes in the SCN of mice showing cyclic expression over 24 h periods. Most of these genes code for the component of the electron transport chain in the mitochondria, substantiating the role of the biological clock in regulating daily energy requirements in the SCN neurons. For the first time, (Simon et al., 2003) reported daily rhythmicity in mitochondrial respiration

in isolated mitochondria from whole-brain homogenates. Further, numerous studies describe the role of the circadian clock in regulating different mitochondrial functions, for example, mitochondrial dynamics (fission-fusion) (Schmitt et al., 2018) and bioenergetics (oxidative phosphorylation and ATP production) (Isobe et al., 2011; Neufeld-Cohen et al., 2016). The mitochondrial redox system is also reported to be clock-controlled through the NAD+-dependent deacetylase SIRT1 (Peek et al., 2013). SIRT1 controls the daily rhythmicity of core clock genes through the deacetylation of the activator and repressor of the core clock machinery (Asher et al., 2008; Nakahata et al., 2008). Genetic ablation of one of the clock activators (Bmal1) resulted in lowered oxygen consumption rate (OCR) in isolated liver mitochondria (Peek et al., 2013; Jacobi et al., 2015). These studies have been performed in the liver, muscle, whole brain tissues, or in-vitro cell lines, which possess independent molecular clocks and show autonomous function. They may be indirectly coordinated by the principal circadian clock (SCN). Peripheral clocks in these tissues are primarily coordinated by non-photic cues like the fasting-feeding cycle or by nutrients (Neufeld-Cohen et al., 2016; de Goede et al., 2022), and are not directly influenced by light. Light is the most powerful cue in resetting the master clock located in the SCN. Although the effects of nutrients and feeding fasting cycle on mitochondrial respiration (Neufeld-Cohen et al., 2016; de Goede et al., 2022) have been extensively studied, to our knowledge, there is no evidence for an influence of lighting conditions on circadian rhythmicity in mitochondrial respiration in the SCN. Based on the above studies, we hypothesize that the biological clock may also regulate mitochondrial bioenergetics to accomplish the metabolic demand by neurons in the SCN.

A recent report indicates that mitochondrial functions like oxidation,

mitochondrial membrane potential, and intracellular calcium holding capacity are regulated by glucocorticoids (e.g., cortisol and corticosterone) (Du et al. 2009). In addition to being a major source of cellular fuel, mitochondria are also the site of synthesis of all steroidal hormones, including glucocorticoid (Bose et al. 2002). In rodents, corticosterone (CORT) is a main glucocorticoid, shows a rhythmic pattern in the LD cycle, and its release is regulated by the central pacemaker (SCN) (Li and Androulakis 2021). CORT level rises before the active phase's onset to prepare the organism for the upcoming stress events throughout the day (Mohawk et al. 2007). Several reports have emphasized the importance of lighting conditions in developing stress responses in rodents and humans. A recent study in mice suggests that light exposure may influence the stress axis both directly and indirectly via circadian system dysregulations (Coleman and Canal. 2017). The effects of LL on the CORT levels in rodents are highly variable. It has been reported by (Fonken et al. 2009; Fonken et al. 2010), that mice exposed to LL showed a higher rate of body weight gain and low levels of corticosterone. Similarly, constant light in C57Bl/6J mice disrupted the CORT rhythm, resulting in lower CORT levels before and after the end of the inactive phase (Coomans et al., 2013). Studies have shown that mean corticosterone levels are increased during the light phase (Claustrat et al., 2008; Tchekalarova et al., 2018). In another study, chronic continuous light exposure sustained increased CORT levels during the subjective light and dark phase (Tapia-Osorio et al., 2013). Based on the above reports, we infer that chronic LL exposure may be a stressful condition for rodents and disrupt CORT's circadian rhythm. It is important to note that studies earlier in LL that resulted in disruption of CORT peak levels have been conducted at two or four-time points of the 24h cycle, which may conceal shifts of acrophases of the CORT rhythm. Therefore, it is essential to evaluate

the circadian profile of CORT in LL to elucidate the disruptive effects of constant light on circulating levels of this major glucocorticoid in rodents.

Together, light is considered the most powerful entraining cue in resetting the circadian clock (SCN). Inappropriately timed light exposure (light pollution) disturbs activity-rest and the fasting-feeding cycle and may disrupt the temporal balance between nutrient supply and energy demand and lead to various pathological conditions, such as increased blood pressure, sleep disorders, breast and prostate cancer, and obesity. Mounting evidence indicates a strong association between chronic dim LL exposure (≤ 5 lux) and dysregulated clock genes rhythms, altered cardiovascular parameters, attenuated locomotor activity patterns, suppressed night-timed melatonin, and disturbed plasma CORT rhythms. Even though extensive research on the detrimental effects of chronic dim light on the circadian clock is evident, the underlying physiological and molecular mechanisms are still not well defined. Therefore, in the present research, we propose to explore the existence of daily rhythms in mitochondrial respiration, variations in the abundance of mitochondrial DNA, and expression of core clock genes involved in regulating such rhythms in the master clock located in the SCN. We also sought to assess the influence of chronic dim LL on such rhythms, the expression of clock genes, and CORT rhythmicity.

## 2.1 Materials and methods

### 2.1.1 Animals and housing

Swiss albino adult male mice (25-30 g, eight-week-old) were procured from the central animal house facility (Institute of Medical Sciences, Banaras Hindu University). They were housed in groups of six in polypropylene cages (41 × 28.2 × 15.3 cm). All the cages were placed in a light and climate-controlled environment

(25±1$^0$C, relative humidity 55±5%, and under 12:12 h light/dark (LD) cycle) for seven days before the start of the experiment. Lighting schedules within the experimental chambers were controlled with the help of an electronic timer (Havells, India). Lights were switched on at 06:00 h Zeitgeber time (ZT0) and were switched off at 18:00 h (ZT 12). Light intensity at the cage floor level was approximately 150 lux (Testo 540) during the day (L) and 0 lux during the night (D). The mice were fed a standard rodent diet (PashuAahar, Varanasi, India). Entry to the experimental chamber for cleaning and providing animal food occurred at random hours, once in 10 days. Food and tap water are provided *ad libitum*. All the experimental protocols were conducted following the principles of laboratory animal care (The Committee for the Purpose of Control and Supervision of Experiments on Animals [CPCSEA], India) guidelines, as well as law approved by the Institutional Animal Ethical Committee (IAEC), Banaras Hindu University (IMS-BHU, No. Dean/2019/IAEC/1254).

### 2.1.2 Experimental design

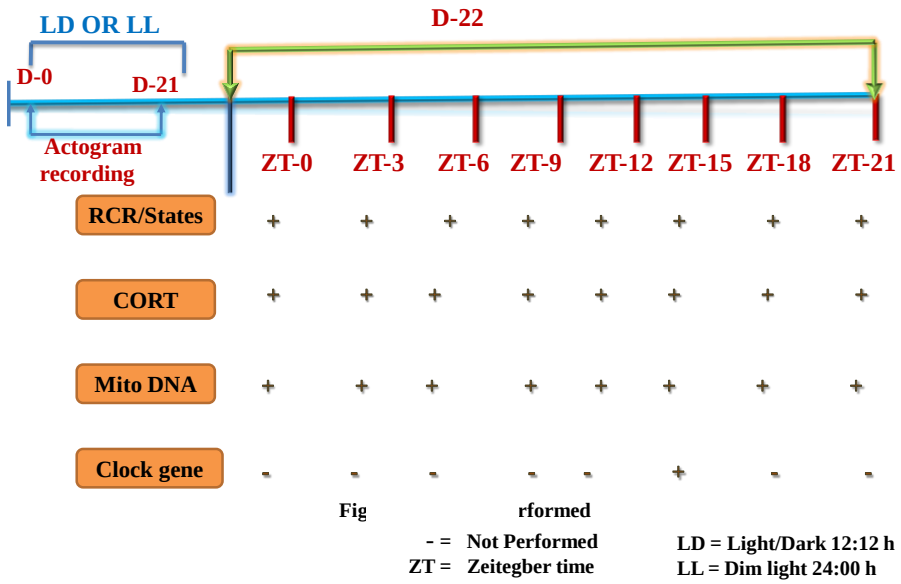


**Figure 2.1 Study design**

After one week of acclimation to 12:12 h LD cycle, mice were weighed and randomly divided into two groups (LD and dim LL, n=192) and transferred to experimental chambers, group first light/dark, 12:12 h LD (L ~150 lux: D = 0 lux, n=96) cycle and group second, chronic dim artificial light for 24 h, LL (L ~ 5 lux: L ~5 lux, n=96). After three weeks under each lighting condition, animals were weighed. Blood and SCN tissues were collected for measurement of mitochondrial respiration (respiratory control rate, RCR), quantitative polymerase chain reaction (qPCR), and mitochondrial DNA (mtDNA), at eight different time points (ZT/CT 0, 3, 6, 9, 12, 15, 18, and 21) over a 24 h cycle.

Blood was collected for CORT analysis over a 24 h period (n = 4/time point). Brains were dissected and SCN was quickly removed and divided into two halves. One-half of the SCN from each animal was stored at -80 ℃ for mtDNA and RNA isolation. Another half of the SCN was immediately processed for mitochondrial bioenergetics analysis (RCR). Three SCN were pooled to make one biological replicate at each time point to isolate mitochondria for RCR and mtDNA/nDNA measurement.

### 2.1.3 Locomotor activity measurement

Healthy adult mice (25-30 g) were singly housed in a polycarbonate cage (11.5 cm width × 21.5 cm length × 30 cm height) equipped with a running wheel in a light and climate-controlled chamber, described above. Wheel running locomotor activity was recorded with the help of a Chronobiology Kit (Stanford Software Systems, Santa Cruz, CA) in 6 min bin size. Both group animals were housed in different experimental chambers with their respective lighting condition. Daily

locomotor activity was recorded till the end of the experiment (three weeks) under both LD and dim LL conditions. Food and water were available *ad libitum* in each cage. Actograms and rhythms were constructed, and the last ten days' data were analyzed using Clock Lab software (version 6.1.10) (Actimetrics, USA). The endogenous period of animals was quantified using a chi-square periodogram (Clocklab functions), and was further verified by following the protocols of (Kumar and Singaravel, 2014).

### 2.1.4 Isolation of mitochondria from brain suprachiasmatic nuclei

The brain was dissected, and coronal hypothalamic sections containing SCN were punched using a gauge needle with an internal diameter of 200 μm. Mitochondria were isolated from the SCN by standard differential centrifugation as per the method of previously described (Berman and Hastings 1999) with slight modifications (Rajput and Krishnamurthy, 2022). Briefly, the brain was dissected, and three SCN were pooled and homogenized in isolation buffer (consisting of 215 mM mannitol, 75 mM sucrose, 0.1 % w/v bovine serum albumin, 20 mM HEPES buffer, and 1 mM of EGTA in 100ml of distilled water and pH adjusted to 7.2 with KOH). They were first centrifuged at 1300 g for 3 min. The supernatant was stored, and the pellet was again centrifuged as above to collect another supernatant. Both the supernatant was mixed and centrifuged at 14,000X g for 10 min at 4°C to get a concentrated mitochondrial pellet.

Further, a washing step was performed by suspending the pellets in the isolation buffer without EGTA and again centrifuged at 14,000X g for 10 min to remove EGTA from the pellets. All the procedures were maintained strictly at 4℃

(Rajput and Krishnamurthy, 2022). Mitochondrial protein was estimated colorimetrically (Lowry et al., 1951) with a microplate reader (BioTek, USA). During preliminary analysis of RCR data, we observed that the mitochondrial concentration in single SCN tissues was too less for detection. Hence, we pooled three SCN samples from three mice (considered as one biological replicate) for measuring RCR. Therefore, four biological repeats from 12 animals per time point were used for the quantification.

### 2.1.5 Measurement of mitochondrial bioenergetics

Mitochondrial respiration was assessed as previously described by (Rajput and Krishnamurthy 2022; Samaiya and Krishnamurthy, 2015), with a Clark-type electrode in a sealed, thermostatically controlled chamber at 37℃. Briefly, the mitochondria were added to the respiratory chamber states were evaluated with suitable substrates and inhibitors. Purified mitochondrial protein was suspended in a respiration buffer in a final volume of 250µL. State II respiration was initiated by adding pyruvate/malate; (P/M) shows a basal respiration rate. The addition of adenosine diphosphate-initiated state III respiration, (ADP); the high level of oxygen utilization indicates that ADP is converted into ATP. The addition of oligomycin measured state IV. The addition of FCCP measured state V. This causes uncoupling of the ETC to ATP synthesis and represents the maximum respiration rate. Rotenone was then added to shut down complex I-mediated respiration. The addition of succinate determined state V. This is the maximum respiration rate via complex II since FCCP is present. The RCR was calculated by dividing state III respiration (presence of ADP) by state IV respiration (absence of ADP).

### 2.1.6 Measurement of mitochondrial DNA

DNA extraction and purification were performed using gMAX Mini Genomic DNA Kit (IBI Scientific), following the manufacturer's instructions with some modifications at different ZTs/CTs after every 3 h over a 24 h period under LD and LL conditions (n = 4 per time point). Briefly, the tissue was introduced into a microcentrifuge tube with 200 µL of GST buffer. Tissue was disrupted using the tissue homogenizer for 4-5s per tissue. Between samples, the tissue homogenizer was rinsed twice with nanopure water. Homogenized samples were then transferred to a new 1.5 mL microcentrifuge tube, and 20 µL of proteinase K (IBI Scientific) was added and incubated for 6 h in a 60 ℃ water bath. Samples were vortex every hour during the 6-h incubation. Following incubation, 200 µL of GSB buffer was added and vortex for 10-sec. RNase A was added, and samples were shaken vigorously and then incubated for 5 min at room temperature to ensure efficient RNA degradation. DNA yield and purity were assessed using the Nanodrop 2000 Spectrophotometer (Thermo Scientific). Real-time quantitative PCR (RT-qPCR) was performed using 200 ng/µl of isolated DNA with the BioRad CFX connect Real-time PCR detection System. TaqMan gene expression assays designed by Thermofisher to target the mitochondrial gene cytochrome B (CYTB; 4331182) and nuclear-chromosomal DNA beta-actin (ACTB; 4352933E) were used for analysis, along with Bullseye TaqProb qPCR master mix (BEQPCR-PS) assay, 2x TaqMan master Mix of dNTPs, Hotstart Taq Polymerase, $Mgcl_2$, Reference dye, and proprietary buffer component, 10Xeach primer, 1XDNA extract (200 ng/ul), and 4X nuclease-free water for a final volume of 20 µl. The PCR temperature cycle used; initial denaturing at 94 °C for 4 min, followed by 45 cycles of denaturing at 94 °C for 30 s, annealing at 60 °C for 30 s, and

extension at 72 °C for 1 min. The ratio of the mitochondrial DNA cycle threshold to genomic DNA was calculated and used to indicate a relative number of mitochondria per cell (Hadsell et al., 2011).

### 2.1.7 Quantification of clock genes expression

Total RNA was isolated from the SCN (*n*=4) tissue at ZT15/CT15, using the TRIzol method (Invitrogen, CA) following the manufacturer's instructions. RNA quality was checked using a Nanodrop 2000 Spectrophotometer (Thermo Scientific) using a 260/280 ratio. RNA (1µg) was converted into cDNA using the Verso cDNA synthesis kit (Thermo Scientific). Quantitative real-time PCR (RTq-PCR) was performed on diluted cDNA samples with SYBR Green JumpStartTaqReadyMix (Sigma-Aldrich), using the CFX Connect real-time PCR System (Bio-Rad, USA). Cycle conditions were used, 50 ℃ for 2 min, 95 ℃ for 10 min, and 40 cycles of 95 ℃ for 15s and 60℃ for 1 min. Relative gene expression of individual samples run in triplicate was calculated by comparison to a relative standard curve and standardized by comparison to the GAPDH signal. The primers were designed using integrated DNA technology (IDT India). Table 2.1 mentions the amplification length and temperature. The primers were validated for linearity and specificity of amplification before the experiment. All reactions were performed in triplicate. The results are expressed relative to a GAPDH, used as an internal control.

**Table 2.1.** List of primers

| Primer name | Primer sequence | Annealing temp. (Tm)$^0$C | Product size(bp) |
|---|---|---|---|
| Clock | F: ACAACGCACACATAGGCCTTC<br>R: TGGTGGTGCCCTGTGATCTA | 57.9<br>58.2 | 21<br>20 |
| Bmal1 | F: CGTGCTAAGGATGGCTGTTC<br>R: CTTCCCTCGGTCACATCCTA | 56.1<br>55.8 | 20<br>20 |
| Per1 | F:TGCACTTCGGGAGCTCAAACTTC<br>R: GTCCATGGCACAAGGCTCACC | 59.7<br>61.0 | 23<br>21 |
| Per2 | F: AACAAATCCACCGGC<br>R: CTCCGGTGAGACTCC | 49.6<br>51.1 | 15<br>15 |
| Cry1 | F: AACGTCCCGAGCTGTAGCGGT<br>R: GACGCTTCCCACTGCTGAGGC | 63.2<br>63.0 | 21<br>21 |
| Cry2 | F: TGCCTCTCCTGCCGCCTCTT<br>R: TGCGGTCCCAGGGGATCTGG | 63.8<br>64.2 | 20<br>20 |
| GAPDH | F: ATCCACTGGTGCTGCCAAG<br>R: CCGTTCAGCTCT GGGATGAC | 58.1<br>57.9 | 19<br>20 |

### 2.1.8 Estimation of corticosterone

To assess the presence temporal rhythms of CORT, blood samples were collected through retro-orbital sinus from mice under LD and LL conditions on the 22 d, at different ZTs and CTs, respectively, ZT/CT 0, 3, 6, 9, 12, 15, 18 and 21 (n = 4 per time point). Blood was collected in heparinized tubes and centrifuged at 3000g for 10 min at 4 °C, and plasma was pipetted and stored at -80 °C for the CORT assay analysis. CORT concentrations were measured in triplicates using high-performance liquid chromatography (HPLC) with an ultraviolet (Diode, UV) detector system (Agilent Technology, USA), according to (Woodward and Emery 1987) with minor modification.

### 2.1.9 Statistical analyses

To determine significant temporal variations in mitochondrial bioenergetics RCR, CORT, and ratio of mitochondrial DNA to genomic DNA, a one-way analysis of variance (ANOVA) was performed. When the data were statistically significant ($p \leq 0.05$), a posthoc Tukey test for multiple comparisons was performed to evaluate the statistical difference between the sampling points (0, 3, 6, 9, 12, 15, 18, 21 and 24) during LD and LL. To quantify the effect of lighting conditions (LD and LL) at maximum response zone on the clock genes expression, data were subjected to a parametric one-tailed student t-test ($p \leq 0.05$). To quantify rhythmicity in the described time series data (RCR, CORT, and ratio of DNA), cosinor analyses were performed by fitting periodic sinusoidal functions to the specific values (via regression analysis by the least-squares method) across the eight-time points using the following equation:$f(t) = M + A\cos(t\pi/12 - \varphi)$, where f(t) is the value of RCR, CORT and mDNA ratio at a given time t to the best-fitted equation, the mesor (M) (rhythm-adjusted mean of the best-fitted cosine curve), amplitude (A) (half the difference between maximum and minimum values of the best-fitted cosine curve), acrophase ($\varphi$) (the time when the peak values of the measured variable occur with reference to local 00:00 h. This procedure is referred to as "single cosinor analysis" (Nelson 1979; Refinetti et al. 2007). Cosinor analysis was used to detect and characterize the percentage of rhythm (percentage of overall variability of data about the arithmetic mean attributable to the fitted rhythmic function) estimates goodness of fit. Further, the F statistic was performed to determine whether the amplitude differs significantly from zero (null hypothesis). The null hypothesis was rejected, and the rhythm amplitude was significantly different from zero (at $p \leq 0.05$, F test). The single

cosinor analysis was performed by the TSA-Time Series Analysis Serial Cosinor 6.3 software (Expert Soft Technologie, Esvres, France). Data analyses and figures were drawn by using Graph Pad Prism 5.0 (La Jolla, CA) and Microsoft Excel 2007 software. Both ZTs and CTs data at time zero is double plotted at ZT/CT 24 to obtain a complete cycle. Data are reported as mean ± SD throughout the text until and unless reported. All experiments were performed as per existing institutional guidelines and in consultation with commonly followed ethical guidelines for biological rhythm research (Portaluppi et al. 2010).

## 2.2 Results

### 2.2.1 Wheel running locomotors activity

Mice under 12:12 LD cycle showed stable and entrained and rhythmic wheel-running locomotor activity patterns (Figure 2.2 A to Figure 2.2 C). The onset of activity was highly precise and showed a positive phase angle difference of approximately 1 h under LD cycle. Activity (alpha) was mostly confined under the dark period (active period), while few bouts of activity were observed during the day (rest period, rho) (Figure 2.2 C). Both alpha (3086.84 ± 481.52) and rho (922.50 ± 485.85) differ statistically ($p < 0.01$) from each other during LD cycle. During chronic dim LL both alpha and rho significantly reduced compared to LD cycle ($p < 0.01$) throughout the experiment (Figure 2D to Figure 2F). After a few days of free-running rhythm, animals became arrhythmic with bouts of activity dispersed both under subjective day and under subjective night (Figure 2.2 D to Figure 2.2 E). There was no significant difference between alpha (408.05 ± 282.56) and rho (253.36 ± 158.60) under dim LL ($p > 0.05$) (Figure 2.2 D and Figure 2.2 F). Importantly, chronic exposure to dim LL disturbed the activity rhythm of animals.

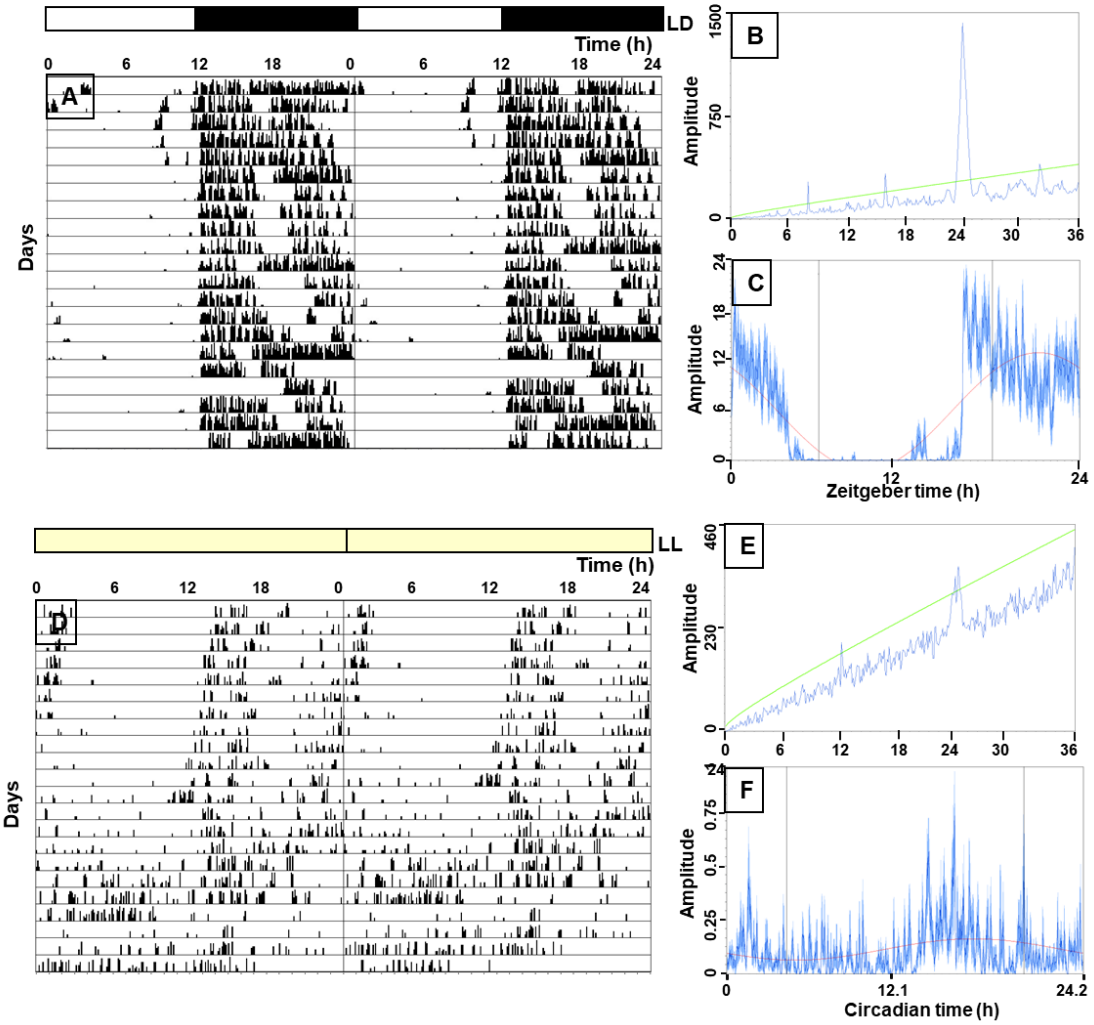


**Figure 2.2**. Wheel running locomotor activity rhythm is in mice is affected by lighting schedule. Representative double plotted actograms depicting the wheel running locomotor activity of mice held under (A) 12:12 h LD and (D) 24:00 h LL, and their periodograms (B) and (E) and activity profiles (C) and (F), respectively. All the three parameters, wheel running rhythm, daily activity profile and periodograms were disrupted by chronic dim LL. Activity pattern under normal LD conditions was rhythmic and robust whereas, it became arrhythmic under dim LL.

### 2.2.2 Respiratory control ratio

To determine the effects of lighting conditions on mitochondrial bioenergetics, we quantified mitochondrial respiration from the SCN-isolated mitochondria in mice raised under LD and LL conditions. Mitochondrial respiration showed strong

interactions between lighting conditions and time of day ($F_{8, 54}$= 10.68, $p < 0.0001$). RCR showed significant temporal variations ($F_{8, 54} = 9.47$, $p < 0.0001$) over the 24 h cycle. The effects of lighting conditions on RCR also varied significantly ($F_{8, 54} = 21.41$, $p < 0.0001$). Under LD condition, one-way ANOVA showed statistically robust variation in mitochondrial bioenergetics ($F_{8, 27} = 20.28$, $p < 0.0001$, Figure 3A), with maximum RCR observed at ZT 12 and minimum at ZT6. During the active period of animals, RCR showed a significant increase. Tukey's post-hoc comparisons show that RCR at ZT 12 and ZT 15 differ significantly with all the time points ($p < 0.0001$) except with each other. Similarly, ZT 18 varied statistically from ZTs 0, 3, 6, and 9 ($p < 0.0001$). RCR was higher even during the late night, at ZT 21 it was significantly higher compared to RCR at ZT 0 ($p < 0.05$), ZT 3 ($p < 0.01$), and ZT 6 ($p < 0.001$) (Figure 2.3A). In contrast, under chronic dim LL, mitochondria respiration was statistically attenuated ($F_{8, 27} = 2.075$, $p > 0.05$, Figure 2.3B).

Also, cosinor analyses showed the presence of significant robust rhythmicity in RCR ($p < 0.0001$) over a 24 h LD cycle compared to RCR in LL. Chronic dim artificial light disturbed the RCR, rhythmicity was lost ($p = 0.575$) and other cosinor parameters were affected by chronic LL. Importantly, both the mesor ($3.18 \pm 0.099$) and amplitude ($1.96 \pm 0.142$) were relatively higher in LD condition compared to LL, mesor ($2.23 \pm 0.2$) and amplitude ($0.28 \pm 0.27$). A significant shift in acrophase was observed during LL, as it shifted from the active phase of mice under LD to the inactive phase (daytime) under LL. Strikingly, a major delay in acrophase of approximately nine hours under chronic dim LL at (ZT24) was observed compared to the acrophase under LD cycle at ZT15 (Figure 2.3C). Thus, chronic LL dysregulated mitochondrial respiration by affecting all the rhythm parameters.

We also explored the influence of dim LL on oxygen consumption in different

states of mitochondrial respiration Table 2.2. We observed that all the states of mitochondrial respiration demonstrate significant temporal variation over a 24 h period similar to RCR, i.e., one-way ANOVA revealed that significant effect of time on mitochondrial respiration, i.e., state 2 ($F_{8, 27}$= 8.45, $p < 0.05$), state 3 ($F_{8, 27}$ = 50.57, $p < 0.05$), state 4 ($F_{8, 27}$ = 110.68, $p < 0.05$), state 5 complex I ($F_{8, 27}$ = 36.43, $p < 0.05$), and state 5 complex II respiration ($F_{8, 27}$ = 45.33, $p < 0.05$) at the different ZTs and CTs. Importantly, during the early rest period (between ZT/CT 0 to ZT/CT 6) under both LD and LL, all the mitochondrial states showed no significant differences in mitochondrial respiration. In contrast, the level of mitochondrial respiration in state 2, state 3 and state 5, gradually started to increase from ZT9 to ZT21 (Supplementary Table 2.2), with a maximum increase in oxygen consumption observed at ZT15 in LD and at ZT18 in LL. On the other hand, in state 4 significant decreases in oxygen consumption were observed between ZT9 to ZT21. The above results indicate that chronic dim LL disrupted mitochondrial states and caused disruption of mitochondrial respiration.

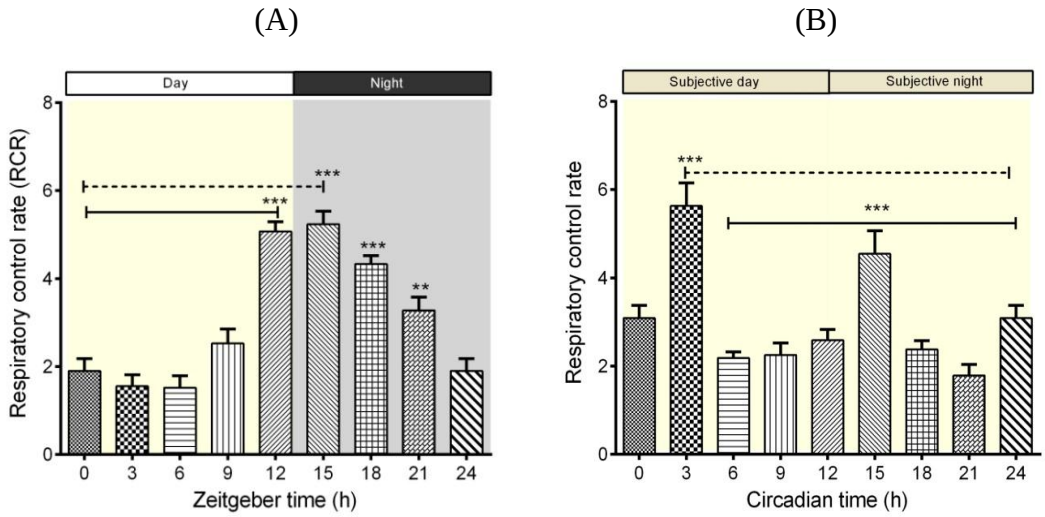


**Figure 2 .3** Temporal variations in mitochondrial respiration in suprachiasmatic nuclei isolated (SCN) mitochondria. (Figure 2.3A) Mitochondrial respiration measured as respiratory control ratio (RCR), increased during the active period of mice, with maximum level at ZT 12 compared to RCR under (Figure 2.3B) chronic

dim LL (maximum at CT 3). Data are represented as mean ± SD (n = 4/time-point) and are considered statistically significant at $p \leq 0.05$.

(c)

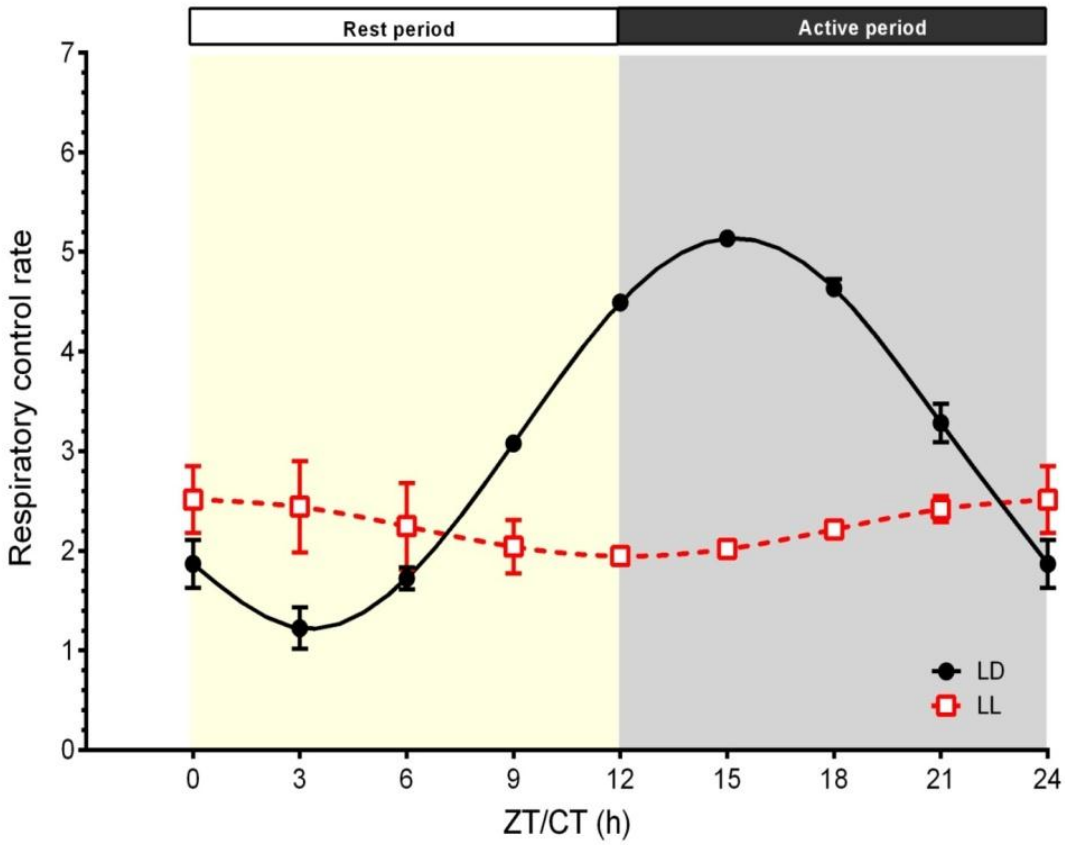


**Figure 2.3C**. Daily rhythms in respiratory control rate (RCR) are influenced by lighting conditions. RCR is highly robust and rhythmic under normal LD, with acrophase during the night (active phase of mice) time (solid black line). Chronic dim LL disrupted the RCR rhythmicity by affecting both amplitude and acrophase over a 24 h period (broken red line). Data are depicted as mean ± SD (n = 4/time-point) and considered to be rhythmic if $p \leq 0.05$ from the non-zero amplitude test (F- test). White and black horizontal bars denote light and dark phase of LD cycle, while yellow horizontal bars depict chronic dim LL condition.

**Table 2.2.** Different mitochondrial respiration states

| Different respiration states | Light condition | Zeitgeber Time Points | | | | | | | |
|---|---|---|---|---|---|---|---|---|---|
| | | **0** | **3** | **6** | **9** | **12** | **15** | **18** | **21** |
| States II (nmol[o]/mg/min) | LD | 6.7 ±0.50 | 6.3 ±0.40 | 6.4 ±0.41 | 16.8 ±1.50$^{a,b,c}$ | 28.9 ±2.40$^{a,b,c,d}$ | 30.6 ±2.50$^{a,b,c,d}$ | 25.4 ±1.58$^{a,b,c,d,e}$ | 19.9 ±2.50$^{a,b,c,d,e,f}$ |
| | LL | 4.2 ±0.50 | 15.2 ±2.50$^{a,*}$ | 4.5 ±1.50$^{b}$ | 4.7 ±1.20$^{b,*}$ | 4.7 ±2.50$^{b,*}$ | 18.7 ±3.10$^{a,b,c,d,*}$ | 5.6 ±1.50$^{b,f,*}$ | 5.1 ±1.10$^{b,f,*}$ |
| States III (nmol[o]/mg/min) | LD | 32.6 ±3.50 | 30.4 ±2.40 | 29.9 ±2.70 | 46.8 ±3.60$^{a,b,c}$ | 81.7 ±3.30$^{a,b,c,d}$ | 84.6 ±4.50$^{a,b,c,d}$ | 67.8 ±3.20$^{a,b,c,d,e}$ | 54.7 ±3.51$^{a,b,c,d,e,f}$ |
| | LL | 23.9 ±2.50$^{*}$ | 64.7 ±5.30$^{a,*}$ | 25.8 ±3.30$^{b}$ | 22.4 ±3.10$^{b,*}$ | 20.2 ±2.70$^{b,*}$ | 67.2 ±5.20$^{a,b,c,d,*}$ | 34.7 ±2.50$^{b,f,*}$ | 32.9 ±3.50$^{b,f,*}$ |
| States IV (nmol[o]/mg/min) | LD | 6.8 ±1.30 | 7.2 ±1.50 | 7.1 ±1.50 | 17.7 ±1.40$^{a,b,c}$ | 27.8 ±2.60$^{a,b,c,d}$ | 29.6 ±2.54$^{a,b,c,d}$ | 23.7 ±2.50$^{a,b,c,d,e,*}$ | 17.6 ±3.50$^{a,b,c,d,e,f}$ |
| | LL | 17.9 ±3.30$^{*}$ | 38.8 ±3.20$^{a,*}$ | 15.6 ±2.30$^{b,*}$ | 19.1 ±3.30 $^{b}$ | 21.8 ±4.30$^{b,*}$ | 41.5 3.40$^{a,b,c,d,*}$ | 18.6 ±2.30$^{b,f,*}$ | 16.9 ±1.30$^{b,f}$ |
| States V (Complex I) (nmol[o]/mg/min) | LD | 35.8 ±4.50 | 31.5 ±4.30 | 32.8 ±3.20 | 50.1 ±4.40$^{a,b,c}$ | 79.9 ±4.20$^{a,b,c,d}$ | 86.7 ±3.30$^{a,b,c,d}$ | 70.2 ±3.30$^{a,b,c,d,e}$ | 49.9 ±2.80$^{a,b,c,d,e,f}$ |
| | LL | 29.8 ±2.10$^{*}$ | 58.7 ±2.00$^{a,*}$ | 27.6 ±2.20$^{b,*}$ | 31.7 ±2.10$^{b,*}$ | 34.2 ±3.50$^{b,*}$ | 62.6 ±4.10$^{a,b,c,d,*}$ | 32.5 ±3.50$^{b,c,*}$ | 30.5 ±2.60$^{b,c,*}$ |
| States V (Complex II) (nmol[o]/mg/min) | LD | 35.4 ±3.60 | 33.6 ±3.40 | 36.5 ±3.20 | 49.6 ±3.67$^{a,b,c}$ | 58.4 ±3.50$^{a,b,c,d}$ | 61.7 ±3.80$^{a,b,c,d}$ | 51.2 ±2.60$^{a,b,c,d,e}$ | 42.9 ±2.90$^{a,b,c,d,e,f}$ |
| | LL | 28.5 ±2.71$^{*}$ | 45.6 ±3.60$^{a,*}$ | 25.1 ±2.60$^{b,*}$ | 26.6 ±2.61$^{b,*}$ | 29.3 ±2.65$^{b,*}$ | 48.4 ±3.60$^{a,b,c,d,*}$ | 33.5 ±2.68$^{b,c,*}$ | 30.4 ±2.62$^{b,c,*}$ |

### 2.2.3. Mitochondrial DNA

We measured the number of mitochondria in the SCN of mice under both LD and LL regimen to determine the cause for disrupted respiratory patterns under chronic dim LL. The number of mitochondria in LD and LL raised mice was measured as the ratio between the copy number of mtDNA and the copy numbers of a nuclear DNA (nDNA). One-way ANOVA showed significant time-dependent effects on the ratio of mtDNA and nDNA under 12:12 h LD cycle ($F_{8, 27} = 36.78$, $p \leq 0.0001$) (Figure 2.4A), showing higher mtDNA copy number during the active period of mice (dark period) with a maximum number at ZT15. Tukey's post-hoc test demonstrated that mitochondrial abundance at ZT15 differs significantly with all the time points ($p < 0.0001$) except with that at ZT12. Similarly, ZT12 also differ significantly from all ZTs except ZT15 ($p < 0.01$). Similarly, mice under chronic dim LL also showed significant effects of time ($F_{8, 27} = 13.93$, $p \leq 0.001$) on the mitochondrial abundance (Figure 2.4B). Tukey's post-hoc comparisons show mitochondrial abundance at ZT15 differs significantly with all the time points ($p < 0.0001$). Similarly, ZT3 varied statistically from ZTs 0, 9, 18 and 21 ($p < 0.0001$). Further, to examine the presence of rhythmicity in the ratio between the mtDNA and nuclear DNA, cosinor analysis was performed. The cosinor analysis revealed significant rhythm (94.99 percent, $p = 0.0001$) under LD (Figure 3 C), with the acrophase observed at ZT15, together with mesor ($10.2 \pm 0.207$) and amplitude ($6.24 \pm 0.294$). This may be due to a higher abundance of mitochondrial DNA during the normal lighting cycle of mice. In contrast, during chronic dim LL the mitochondrial abundance rhythm was disrupted (16.26 percent, $p = 0.119$) (Figure 2.4 C). Also, both mesor ($4.81 \pm 0.379$) and amplitude ($1.1 \pm 0.51$) were significantly dampened by chronic dim lighting regimen.

LL may have acted as a stressor and may have lowered the mitochondrial number. Furthermore, to assess if there is any relationship between mitochondrial abundance and mitochondrial respiration and the influence of lighting conditions on them, correlation analyses between RCR and mtDNA/nDNA under LD and LL were performed. We observed that the mitochondrial respiration and mtDNA/nDNA was highly correlated under LD ($r^2$=0.95, p=0.0001) conditions (figure 2.4D). In contrast, such correlation under chronic dim LL appeared to be weak ($r^2$= 0.53, p=0.02, figure 2.4E). Thus, chronic dim LL resulted in dysregulated mitochondrial abundance compared to LD.

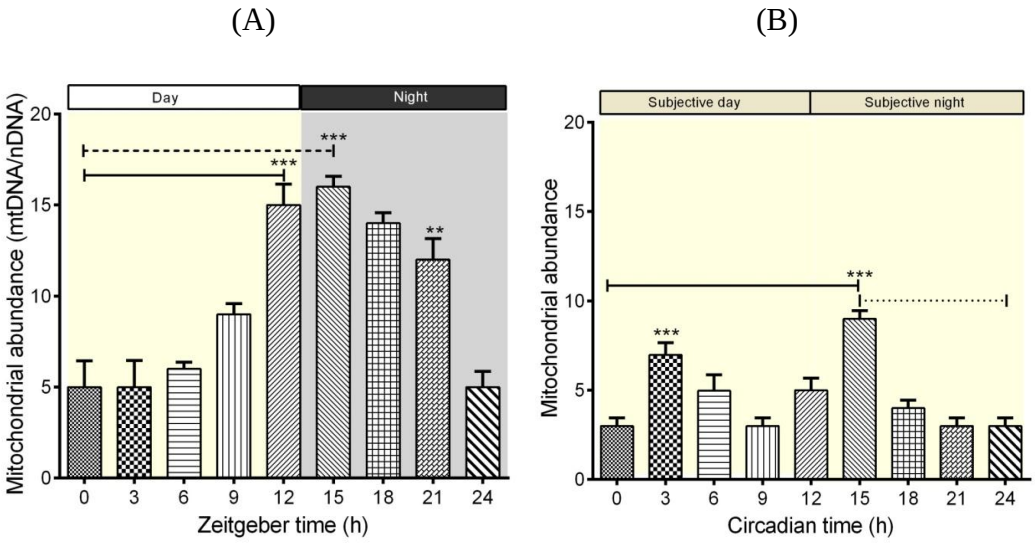


**Figure 2.4**. Daily fluctuation in mitochondrial copy number (mtDNA/nDNA ratio) over a 24-h period. (Figure 2.4A) Mitochondrial abundance was significantly higher during the active phase of mice (night), with maximum number at ZT15. (Figure 2.4B) During dim LL, mitochondrial abundance was dysregulated. Data are shown mean ± SD (n= 4/time-point), and considered statistically different at $p \leq 0.05$.

(C)

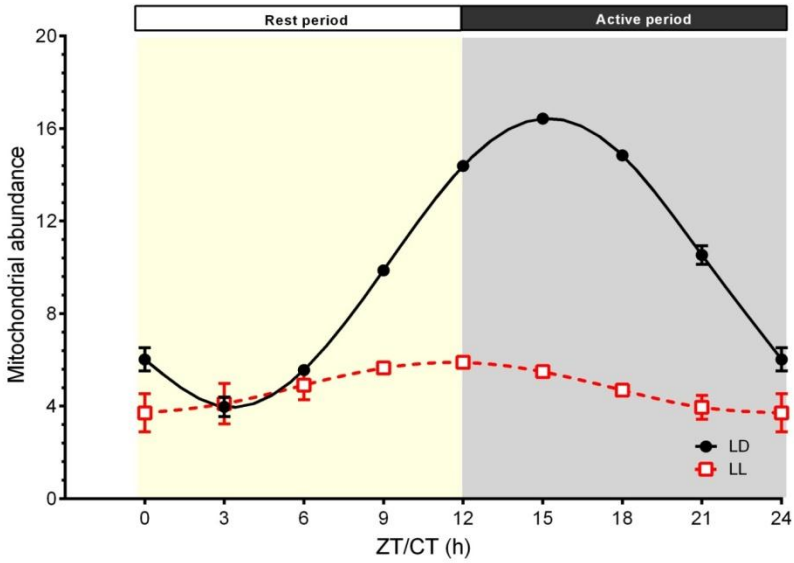


**Figure 2.4C**. Daily rhythms in mitochondrial abundance (mtDNA/nDNA ratio) are affected by lighting conditions. mtDNA/nDNA ratio is strongly robust and rhythmic under normal LD conditions, with a peak (acrophase) during the night time at ZT15 (solid black line). Chronic dim LL disturbed the rhythmicity of mitochondrial abundance by influencing the amplitude and acrophase over a 24 h period (dashed red line). Data are depicted as mean ± SD (n = 4/time-point). Data is considered to be rhythmic if $p \leq 0.05$ from the non-zero amplitude test (F- test). White and black horizontal bars denote light and dark phase of a 24 h period. Solid black line depicts cosinor data under LD and dashed red line denotes cosinor data under chronic dim LL.

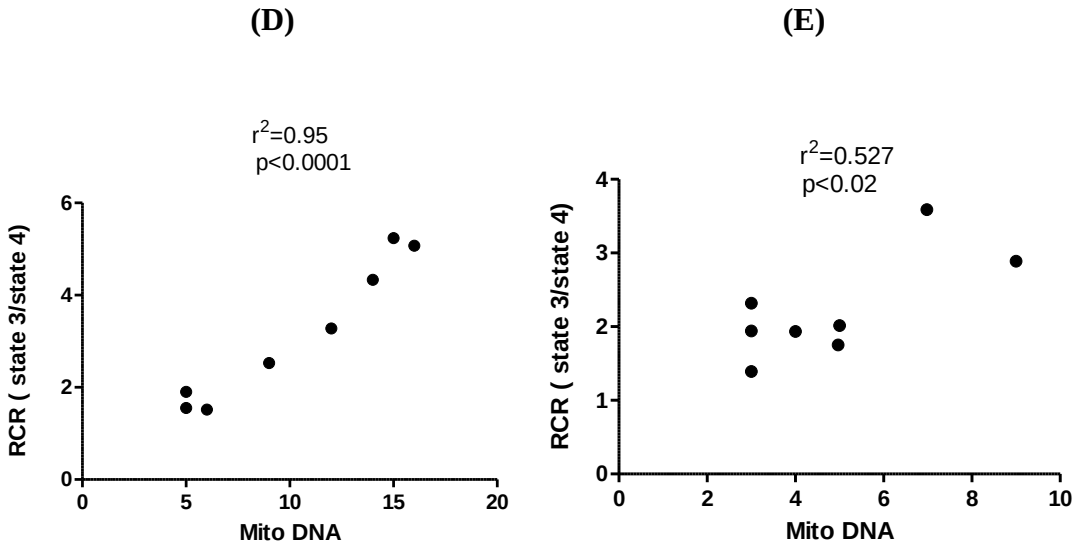


**Figure 2.4 (D)** correlation analysis of RCR and Mito DNA in LD 12:12 h and **(E)** LL 24:00 h. (n=4). $p \leq 0.05$ considered as statistically significant.

### 2.2.4 Clock genes

Expression of core clock genes in the SCN was quantified at the maximum responsive zone, ZT/CT15 (during the active period of mice), where maximum RCR and CORT levels were observed. We wanted to determine the effects of lighting conditions on clock gene expression levels and their relationship (if any) in the regulating respiratory rate of the principal clock and also on the blood CORT levels. Student's t-test showed significant effects of lighting conditions on the expression levels core clock genes (*Clock, Bmal1, Cry1, Cry2, and Per1, Per2*) in the SCN. Compared to LD condition, continuous light exposure significantly ($p \leq 0.001$) down regulated (by 1.3 to 1.9 fold, Figure 2.5), the levels of all the clock genes.

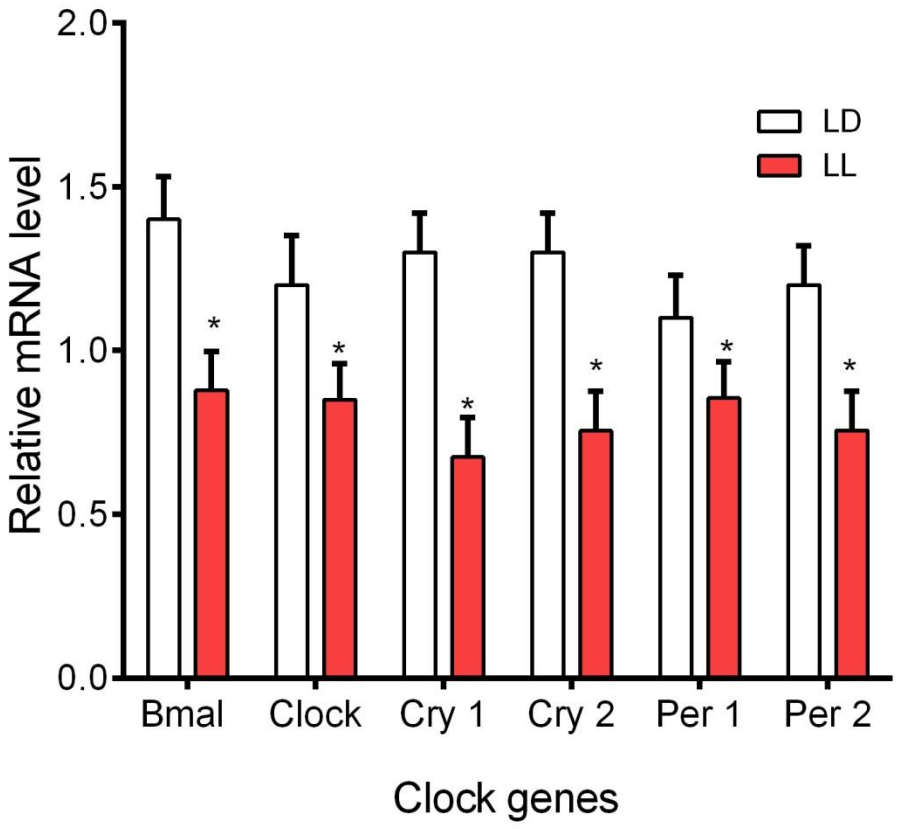


**Figure 2.5** Relative abundance of mRNA expression of core clock genes from SCN tissues was significantly influenced by chronic dim LL at ZT/CT15 of a 24 h periodic cycle. All the clock genes under LD cycle differed more than 1.2-fold from its

expression under dim LL. Data are shown as mean ± SD (n = 4/time point), and regarded as statistically significant, if $p \leq 0.05$ (one tailed t test)

### 2.2.5 Corticosterone level

To assess the impact of lighting manipulation on the plasma CORT rhythms and its levels, we estimated the CORT at different time points of 24 h period. Two-way ANOVA analysis demonstrated a significant interaction ($F_{8, 54} = 62.27$, $p < 0.0001$) between light and time (ZT/CT) on daily plasma CORT levels in mice (Figure 2.6A and B). Manipulation of lighting conditions statistically affected ($F_{1, 54} = 5.67$; $p = 0.021$) the levels of CORT. Also, significant effects of time ($F_{8, 54} = 45.98$, $p < 0.0001$) on 24 h plasma CORT levels were noticed. Under LD, one-way ANOVA demonstrated that CORT show a significant temporal variation over a 24 h LD cycle, ($F_{8, 27} = 366.20$, $p < 0.0001$), with higher concentration observed during the night (active period). The maximum CORT level was estimated at ZT0, and the levels remained relatively lower until ZT12. Tukey's multiple comparisons show that CORT at ZT0, ZT6, and ZT15 differ statically from all the phases' $p < 0.01$). The level of CORT at ZT3 varied significantly from ZT18 ($p < 0.001$). Similarly, CORT at ZT9 shows significant difference ($p < 0.01$) in its levels compared to all the ZTs except ZT12 and ZT21 (Figure 2.6A). Similarly, under LL, one-way ANOVA showed that CORT varied significantly over a 24 h period ($F_{8, 27} = 20.03$, $p < 0.001$), with maximum levels at CT21. Post-hoc comparisons indicated that CT18 and CT21 differ significantly ($p < 0.001$) from all the CTs. Importantly, compared to LD, the CORT levels remained relatively high and flattened throughout the subjective day and early subjective night. However, for short duration (between CT18 and CT 21) its level increased during late subjective night (Figure 2.6B).

Further, cosinor analysis indicates that light conditions affect the rhythm parameters of CORT. Mice exposed to LD showed statistically robust rhythmicity in plasma CORT ($p < 0.001$), with acrophase at ZT 22.52, mesor = 10.8, and amplitude = 5.8 (Figure 2.6C). In contrast, although CORT showed rhythmicity ($p < 0.05$) under LL, it was fairly weak compared to LD condition, and the acrophase was observed at CT 19, mesor = 11.1, amplitude = 2.4. Strikingly, the LL affected the amplitude as well as the phase of the acrophase of CORT.

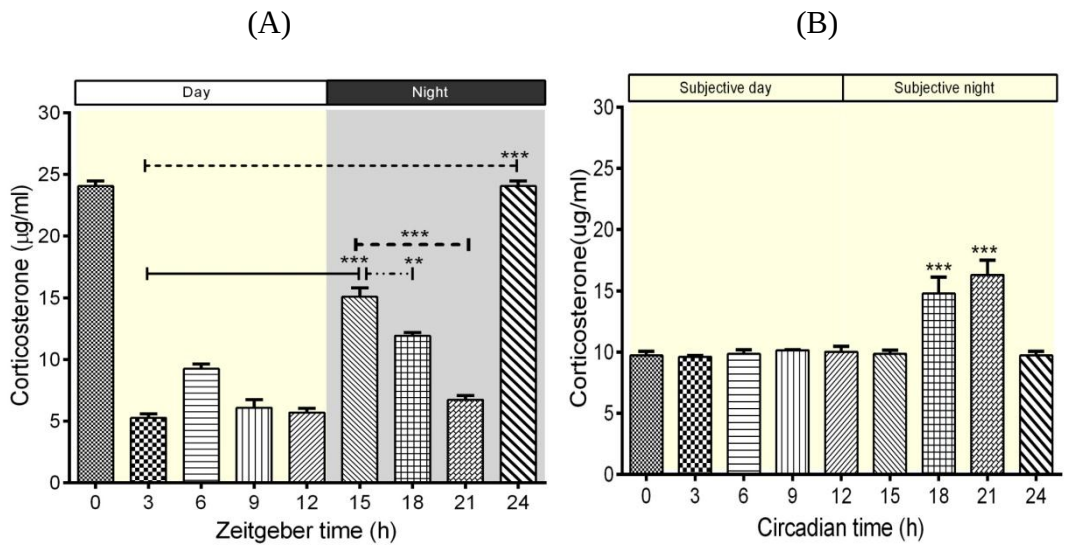


**Figure 2.6**. Plasma corticosterone levels are disrupted by chronic dim LL. (Figure 2.6A) shows CORT level significantly increased during the dark period with maximum level at ZT 24 under LD cycle. (Figure 2.6B) depicts that chronic dim LL resulted in flattened CORT levels throughout subjective day (CT0 to CT12) and early subjective night (CT12 to CT15) compared to LD conditions, except at CT18 and CT21. Data represented as mean ± SD (n = 4/time-point) and are significant if $p \leq 0.05$.

(C)

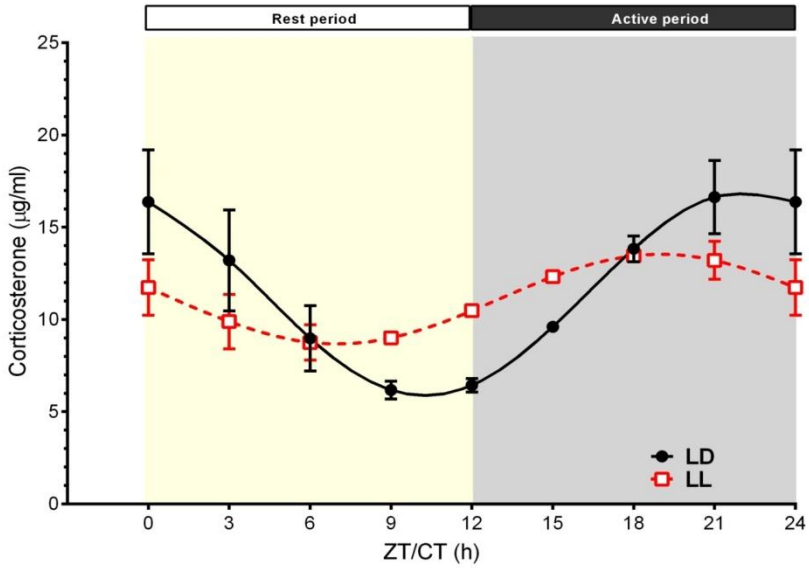


**Figure 2.6 C**. Daily rhythms of plasma CORT levels measured over a 24 h period in mice under different lighting conditions (LD and dim LL). Plasma CORT showed strong rhythmicity under LD cycle (solid black line). In contrast, CORT rhythmicity was altered and shift in the acrophase was observed (red dashed line). Data under LD and LL are denoted as the best least squares approximating cosine curve fitted to CORT level over a 24 h period. White and black horizontal bars depict duration light and dark phase over a 24 h LD cycle. Data are represented as mean ± SD, (n = 4/ time point). $p \leq 0.05$ from the non-zero amplitude test.

## 2.3 Discussion

In the present study, our results demonstrate the existence of a robust daily rhythmicity in mitochondrial respiration in the SCN (principal circadian clock) of mice and substantiate the role of the biological clock in controlling mitochondrial functions. Further, chronic exposure to dim artificial light abrogated this daily rhythmicity in locomotor activity rhythm, mitochondrial respiration, mtDNA/nDNA temporal pattern, and dysregulated core clock gene expression levels, and disrupted the daily CORT rhythm.

Mice under normal 12:12 LD cycle showed robust entrained locomotor

activity rhythm, with major activity during their active period (night). In contrast, mice under chronic dim LL initially displayed a free running locomotor activity rhythm with an endogenous periodicity of more than 24 h. However, a week later, mice displayed arrhythmic wheel-running locomotor activity behavior. Our behavioral results are in agreement with previously published reports in rats, describing that constant light leads to the progressive development of arrhythmic locomotor rhythms (Depres-Brummer et al. 1995; Tapia-Osorio et al. 2013). Such arrhythmicity in activity patterns as a result of constant lighting has been compared with the results observed in rats with lesioned SCN (Chiesa et al. 2010). Our periodogram data, together with plasma CORT results, which showed disrupted rhythmicity in mice under dim LL, further corroborates the results of an aforementioned study. Present data are further are supported by a study describing the arrhythmicity in several metabolic markers and CORT rhythm in rats exposed to dim light (Dauchy et al., 2010).

The present results reveal a strong link between the lighting condition and mitochondrial bioenergetics in the SCN. We show that untimed exposure to artificial dim light results in mitochondrial dysfunction and altered respiration. Mice under normal LD cycle showed robust daily rhythm in mitochondrial bioenergetics, whereas chronic exposure to dim LL strongly dampened the amplitude of this rhythm and reduced the overall 24 h respiration rate. This indicates a possible disruptive role of chronic dim LL in regulating mitochondrial functions in the SCN. Numerous studies have shown the existence of similar rhythms (daily) in mitochondrial respiration both in in-vivo and in vitro. However, these studies have been performed in the liver, cardiac muscle (Bray et al. 2008), skeletal muscle (de Goede et al., 2022; Neufeld-

Cohen et al., 2016; Peek et al., 2013; van Moorselet et al., 2016), or whole brain tissues (Simon et al., 2003) or on the in-vitro cell lines (Peek et al., 2013, 2015; Rabinovich-Nikitinet et al., 2021), which have their own clock machinery and may show autonomous function or may be indirectly coordinated by the principal circadian clock (SCN). These peripheral tissues are reported to be synchronized primarily by the fasting-feeding cycle or by the presence of nutrients and are not directly affected by light.

In contrast, light is the most potent cue in resetting the principal clock located in the SCN. This may in turn, regulate the several peripheral oscillators within the brain or down to the heart, kidney, liver, and muscles. Daily rhythms of mitochondrial respiration in the above studies are reported to be higher during the active phase of animals. Similarly, our results show that mitochondrial respiration is rhythmic under 12:12 h LD condition with maximum amplitude at ZT15, 3 h after lights off (active phase of mice), and minimum at ZT3. Similarly, our results show that mitochondrial respiration is rhythmic under 12:12 h LD condition and remains elevated throughout the night with maximum amplitude at ZT15, 3 h after lights off (active phase of mice), and minimum at ZT3. Surprisingly, artificial dim LL markedly dampened the amplitude of RCR and altered its rhythmicity (Figure 2 A and B). Thus, chronic dim LL disrupts the principal clock and leads to impaired mitochondrial respiration in the SCN. Thus, lighting conditions influence RCR and regulate the proper functioning of the master clock in the SCN. We propose that similar to mitochondrial respirations in the liver and muscles (Neufeld-Cohen et al., 2016; de Goede et al., 2022), several catabolic enzymes might be involved in regulating oscillations in mitochondrial respirations in the SCN. Exposure to dim LL may disrupt these enzymes and may

influence the proper functioning of SCN, causing altered rhythmicity in mitochondrial respiration of the principal clock.

Similar to RCR during LD and LL, mitochondrial abundance was also disturbed due to chronic dim LL. Strikingly, the mitochondrial abundance was significantly reduced during LL compared to their numbers under LD (Figure 3A and 3B) conditions. Thus, dim LL acts as a stressor for the mitochondria in the SCN of mice. Such decreased mitochondrial abundance indicates that chronic dim LL may have caused a mutation in the mitochondrial genome due to stress and would have resulted in disturbed mitochondrial proteins or several other factors regulating mitochondrial function, for example, fission and fusion (dynamics), membrane potential (de Goede et al., 2022). Disturbances in aforementioned mitochondrial functions may have also lowered respiratory rate. In the LD-reared mice, mitochondrial abundance appeared to be statistically rhythmic compared to that in LL (arhythmic), demonstrating the importance of time and duration of light exposure on the normal functioning of mitochondrial physiology. Another possible reason for depressed mtDNA/nDNA may be that chronic dim LL may have disturbed the feeding-fasting schedule that may have dysregulated the balances in mitochondrial biogenesis, mitophagy, and dynamics, leading to atypical mitochondrial abundance rhythm over a 24 h period (Mauri et al., 2022). Our idea is supported by a study that shows the importance of mitochondrial genomic stability on mitochondrial respiration (Stuart and Brown 2006). Any disturbances to mtDNA due to oxidative stress as a result of chemical oxidants (Mambo et al., 2003), and ionizing radiation (Chan et al., 2002) are reported to cause mutation in the mtDNA and may hamper several mitochondrial functions.

To further provide a mechanistic understanding of the cause for the lower respiration and dampened rhythmicity in the dim LL exposed mice, core clock gene expression levels in the SCN were investigated. Under chronic dim artificial lighting, the levels of the clock genes (both activator and repressors) expression were downregulated (1.2 to 1.9-fold) during the active period of mice at (CT15) compared to mice under LD condition at (ZT15) (Figure 4). During these time zones, maximal variation in the level of mitochondrial bioenergetics as well as the ratio of mtDNA/nDNA, was observed in our study. These results confirm that chronic dim LL disrupts the core circadian clock, leading to impaired mitochondrial bioenergetics and disturbed mitochondrial gene expression. Our results are substantiated by several studies describing the role of the circadian clock in regulating several mitochondrial functions, for example, dynamics (fission-fusion) and bioenergetics (oxidative phosphorylation and ATP production) (Isobe et al. 2011; Neufeld-Cohen et al. 2016; Panda et al. 2002) reported more than 300 genes in the SCN of mice showing cyclic expression over 24 h period. In addition, BMAL1 is reported to control reactive oxygen species generation by affecting morphological changes in mitochondria (Jacobi et al. 2015). The mitochondrial redox system is linked to the biological clock through the NAD+-dependent deacetylase SIRT1. SIRT1 causes deacetylation of the clock activator (BMAL1) and repressor (PER2) affecting the daily rhythmicity of core clock genes (Asher et al. 2008; Nakahata et al. 2008). Further, the deletion of Cry1 and Cry2 genes, a repressor of BMAL1/CLOCK, resulted in an elevated mitochondrial reserve capacity in primary myotubes and improved work performance in mice (Jordan et al., 2017). Mice with whole-body Bmal1 mutation showed decreased RCR (Andrews et al., 2010; Peek et al., 2013), causing impaired

respiration. Likewise, whole-body abrogation of the Reverba (accessory clock component) in mice affected the state 3 respiration in isolated mitochondria as well as in soleus muscle fibers (Woldt et al., 2013). Thus, our present data together with aforementioned reports confirm the role of the core molecular clock in regulating energy production in SCN to compensate for increased metabolic requirements during the active phase of organisms. Further, untimed exposure to artificial light disrupts the principal molecular clock (SCN), which is supported by several light phase response curve studies in both diurnal and nocturnal mammals (Comas et al., 2006; Kumar and Singaravel 2014), and may be one the reason for abnormal mitochondrial rhythmicity and altered respiration under dim LL.

Also, the report suggests that mitochondrial functions like oxidation, mitochondrial membrane potential, and intracellular calcium holding capacity are regulated by glucocorticoids (e.g., cortisol and corticosterone) (Du et al., 2009). In addition to a major source of cellular fuel, mitochondria are also the site of synthesis of all steroidal hormones, including glucocorticoid (Bose et al., 2002). In our study, the mean corticosterone level in LL is relatively flat and higher in concentration during the subjective day and early subjective night (CT 0 to CT 15) compared to CORT levels in mice under LD cycle (Figure 5 A and B) early night and during the transition from night to day. In LD, the CORT levels gradually increase during the active period after the lights off. Our data partially agree with the results of several studies under chronic LL conditions (Claustrat et al., 2008; Tapia-Osorio et al., 2013; Tchekalarova et al., 2018), where they have shown that the mean plasma CORT levels are relatively high during the subjective light phase of animals (inactive period) compared to the subjective dark (active period). This suggests that chronic LL may act a stressor, disrupting the daily rhythm of plasma CORT in animals as a result of an

abnormal increase in its levels during the inactive period of animals. Such disturbance may have been because of disturbed sleep-wake and feeding-fasting cycle, causing animals to eat during their resting phase (subjective day). Such abnormal feeding rhythms may have triggered increased metabolic activity, leading to activation demand of the HPA axis to produce more CORT during the subjective day. Our notion is supported by a recent study in mice in which LL causes an immediate increase in body weight compared to mice exposed to LD cycle (Coomans et al., 2013).

In contrast, in several other studies, level of CORT have significantly decreased during LL **(**Coleman and Canal 2009; Fonken et al., 2009; Fonken et al., 2010), indicating that LL shows the highly diverse effect on CORT level in rodents. It is noteworthy that most of the data outlined in the above studies have assessed CORT at either at two-time points or four-time points of 24 h period. Such fragmented estimation may not display the actual variations over the complete 24 h period and may fail to detect several important cosinor parameters like the amplitude, mesor and the phase of acrophase of any rhythm (CORT). In our study, even though the CORT was rhythmic under LL, the amplitude was dampened (A = 2.43), and most importantly, the acrophase was phase advanced by 3 h compared to that under LD condition (A= 5.53.φ = 22h 52 min). Thus, LL shows diverse effects on the CORT levels that are observed to differ between the species and the strains.

## 2.4 Summary

In summary, robust rhythmicity exists in mitochondrial respiration and abundance even in the SCN and plasma CORT under a normal LD cycle. However, chronic dim LL exposure altered these rhythms and dysregulated the expression levels of core clock genes. This suggests that the circadian clock controls mitochondrial

functions (respiration, number), crucial for fulfilling daily energetic demands by the SCN neurons. Chronic dim artificial LL disrupts such strong coordination between the clock and the mitochondria in the SCN and between the clock and hormone (CORT), resulting in altered mitochondrial functions in the SCN, which may disturb metabolism, causing obesity, diabetes, and other metabolic disorders. Thus, it is important to consider appropriate lighting conditions (intensity, duration, and wavelengths) in workplaces.